CODEN IEJMAT *Internet Electronic Journal of Molecular Design* **2006**, *5*, 447–459 ISSN 1538–6414
BioChem Press http://www.biochempress.com

Inter*net* Electronic Journal of Molecular Design

August 2006, Volume 5, Number 8, Pages 447–459

Editor: Ovidiu Ivanciuc

Special issue dedicated to Professor Lemont B. Kier on the occasion of the 75th birthday

Electronic Structures of Heme(Fe)–Dioxygen Complex as an Intermediate Model of Dioxygen Reduction in Cytochrome *c* Oxidase

Yasunori Yoshioka,[1] Masaki Mitani,[1] and Hiroyuki Satoh [1]

[1] Chemistry Department for Materials, Graduate School of Engineering, Mie University, Kurima–Machiya 1577, Tsu, 814–8507 Japan

Received: April 24, 2006; Revised: June 5, 2006; Accepted: June 15, 2006; Published: August 31, 2006

Citation of the article:
Y. Yoshioka, M. Mitani, and H. Satoh, Electronic Structures of Heme(Fe)–Dioxygen Complex as an Intermediate Model of Dioxygen Reduction in Cytochrome *c* Oxidase, *Internet Electron. J. Mol. Des.* **2006**, *5*, 447–459, http://www.biochempress.com.

Inter*net* Electronic Journal of Molecular Design

BioChem Press
http://www.biochempress.com

Electronic Structures of Heme(Fe)–Dioxygen Complex as an Intermediate Model of Dioxygen Reduction in Cytochrome *c* Oxidase

Yasunori Yoshioka,[1,*] Masaki Mitani,[1] and Hiroyuki Satoh [1]

[1] Chemistry Department for Materials, Graduate School of Engineering, Mie University, Kurima–Machiya 1577, Tsu, 814–8507 Japan

Received: April 24, 2006; Revised: June 5, 2006; Accepted: June 15, 2006; Published: August 31, 2006

Internet Electron. J. Mol. Des. **2006**, *5* (8), 447–459

Abstract

Motivation. We have previously proposed the O_2 reduction mechanism that the protons transfer from the K–channel to the active site of C*c*O. The second proton transfer to the hydroperoxy intermediate FeOOH did not lead the OO bond cleavage. It has been recently reported that the addition of the proton induces the OO bond cleavage to yield the productive H_2O molecule and the oxo intermediate Fe=O, being inconsistent with our results. We have started this study to confirm whether the OO bond cleavage occurs or not upon the proton addition. We concentrated our study to the changes of the electronic structures of the heme a_3 part throughout the sequential additions of the protons and an electron during the process of the O_2 reduction.

Method. We employed a model that is composed of porphyrin without any substituents, Fe, and an imidazole as His376. We added sequentially protons and an electron to the heme(Fe)–dioxygen complex. The geometrical parameters were fully optimized without any constraints. The unrestricted hybrid exchange–correlation functional B3LYP method was used. The Wachters double zeta basis set was employed for Fe atom. The 6–31G* basis set was used for C, N, and H atoms, and the 6–311+G* for O atom. All calculations were carried out using the program package Gaussian 98.

Results. The proton addition to FeOO (**H2**) to yield FeOOH (**H3**) causes the electron transfer from the porphyrin ring to FeOOH moiety, giving the porphyrin–radical cation. The additional proton to FeOOH (**H4**) leads to the OO bond cleavage, yielding the hydrogen bonded complex of an oxo heme (compound I) and a H_2O molecule. The bonding characters of FeOOH in **H3** and **H4** are identical, even though the electronic structures of the porphyrin rings in **H3** and **H4** are different. However, the proton addition to FeOOH (**H3**) does not lead to the OO bond cleavage.

Conclusions. The protonated heme(Fe)–dioxygen complexes are effective models to investigate the reduction mechanism of a O_2 molecule in C*c*O.

Keywords. Cytochrome *c* oxidase; heme; electron transfer; B3LYP.

Abbreviations and notations

C*c*O, cytochrome *c* oxidase	Por, porphyrin
Imz, imidazole	

Dedicated to Professor Lemont B. Kier on the occasion of the 75th birthday.

* Correspondence author; phone: 81–59–231–9742; fax: 81–59–231–9742; E–mail: yyoshi@chem.mie–u.ac.jp.

1 INTRODUCTION

The Cytochrome *c* oxidase (C*c*O) is known to proceed the reduction of oxygen molecule to water molecules with electron transfer from cytochrome *c* and proton pumping from the matrix side of the mitochondrial membrane toward the cytosolic side [1–3]. The active sites of both fully reduced and oxidized states of bovine heart enzyme are composed of binuclear, heme a_3 and Cu_B [4–7]. Heme a_3 has a ligand of imidazole from His376, and Cu_B has three ligands of imidazoles from His 240, His290, and His291. His240 is cross–linked to Tyr244 with a covalent bond (Figure 1).

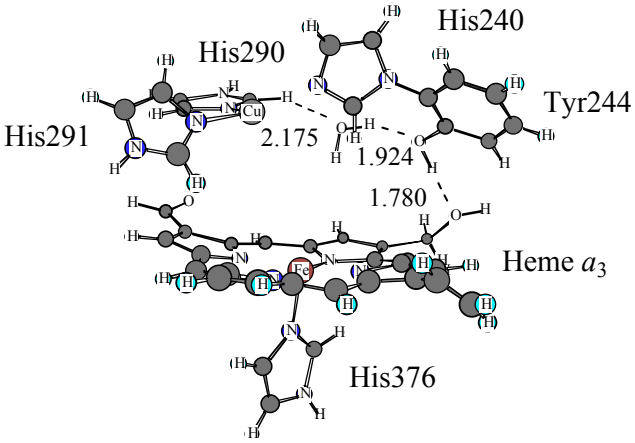

Figure 1. Model of active site in fully reduced form C*c*O (1OCR in PDB). H_2O molecule is hydrogen–bonded to both His290 and Tyr244.

The O_2 molecule in the triplet state is initially bound to Fe atom of heme a_3 in the reduced form, [Fe(II), Cu(I)], to yield the oxy intermediate [FeOO, Cu] [2,3,8,9]. The subsequent intermediate observed experimentally is the oxo intermediate [Fe=O, Cu] [3,8–14]. There is now consensus that first two protons are provided from the K–channel that begins from Lys319 and ends to Thr316 [15,16]. In our previous papers [17], it has been shown that a H_2O molecule shown in Figure 1 is hydrogen–bonded to both Tyr244 and His290, and is a key molecule to produce FeOOH. This H_2O molecule plays a crucial role as a carrier of a proton toward FeOO to yield [FeOOH, Cu]. The Cu atom is formally changed from the cuprous state to the cupric state through transportation of a proton by the H_2O molecule. It has been also shown that the proton to yield FeOOH is trapped on farnesylethyl of heme a_3, and is subsequently transferred to Tyr244 to give a proton to the H_2O molecule between His290 and Tyr244 [18]. The energy barrier of the proton transfer was qualitatively estimated to be 12 kcal/mol.

Our proposal of the reduction mechanism of O_2 molecule at the early stage of the reaction could be drawn schematically as shown in Scheme 1 (A). The oxy intermediate [FeOO, Cu], C*c*O**1**, is changed to [FeOOH, Cu], C*c*O**2**, with the proton transfer from the K–channel as described above, and at same time Cu is changed from cuprous to cupric with the electron transfer from the Cu atom

to the porphyrin ring. Subsequently, C*c*O**2** is changed to C*c*O**3** by the electron transfer from heme *a*. As a next step, the proton transfers through the same route of the K–channel to yield a [$FeOOH_2$, Cu]. The distance of the resulting OO bond was estimated to be 1.484 Å [19], showing no OO bond cleavage.

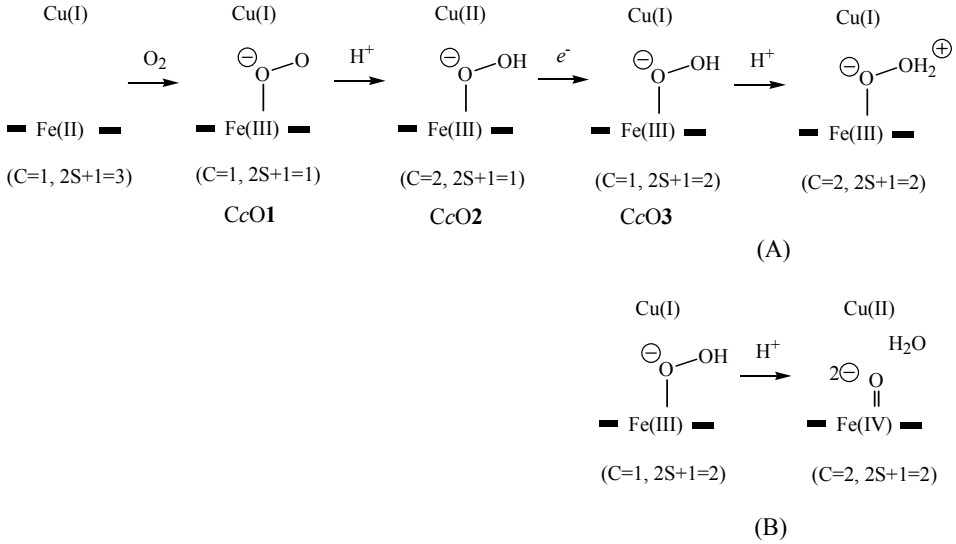

Scheme 1. Schematic representation of mechanism for O_2 reduction to H_2O molecule in the active site of CcO. (A) Our proposal based on the theoretical work [17–19]. (B) Experimental proposal [20].

In a recent publication [20], Faxén and co–workers have shown that the addition of a proton to hydroperoxy intermediate FeOOH induces the OO bond cleavage to yield a productive H_2O molecule and an oxo intermediate Fe=O, such as shown in Scheme 1 (B). These conflicting results drive us to the reinvestigation of our O_2 reduction mechanism.

In this study, we concentrate our study to the changes of the electronic structures of the heme a_3 part throughout the sequential additions of the protons and an electron during the process of the O_2 reduction. The model examined here is composed of porphyrin without any substituents, Fe, and an imidazole as His376. It is first shown that the heme model used here qualitatively reproduces the electronic structures of C*c*O**1**, C*c*O**2**, and C*c*O**3**. It is subsequently found that the proton addition to FeOOH leads the OO bond cleavage.

2 MATERIALS AND METHODS

2.1 Model

In the previous study [17,18], the model of the active site of C*c*O was constructed based on the structure of the X–ray crystallographic study (1OCR in PDB). Shown in Figure 1 is the model constructed in the previous study. The reduction of the O_2 molecule proceeds between Fe in heme a_3 and Cu_B. Figure 2 shows the heme model examined in this study with the coordinate system

employed here. The model is composed of porphyrin without any substituents, Fe, and an imidazole as His376.

2.2 Calculation Procedure

The total charge of the **H1** is neutral, corresponding to [Fe(II), Cu(I)] of the reduced active site of C*c*O. The geometrical parameters were fully optimized without any constraints. We employed the unrestricted hybrid exchange–correlation functional B3LYP [21–24] method. The Wachters double zeta basis set [25] was employed for Fe atom. The 6–31G* basis set was used for C, N, and H atoms, and the 6–311+G* for O atom. All calculations were carried out using the program package Gaussian 98 [26].

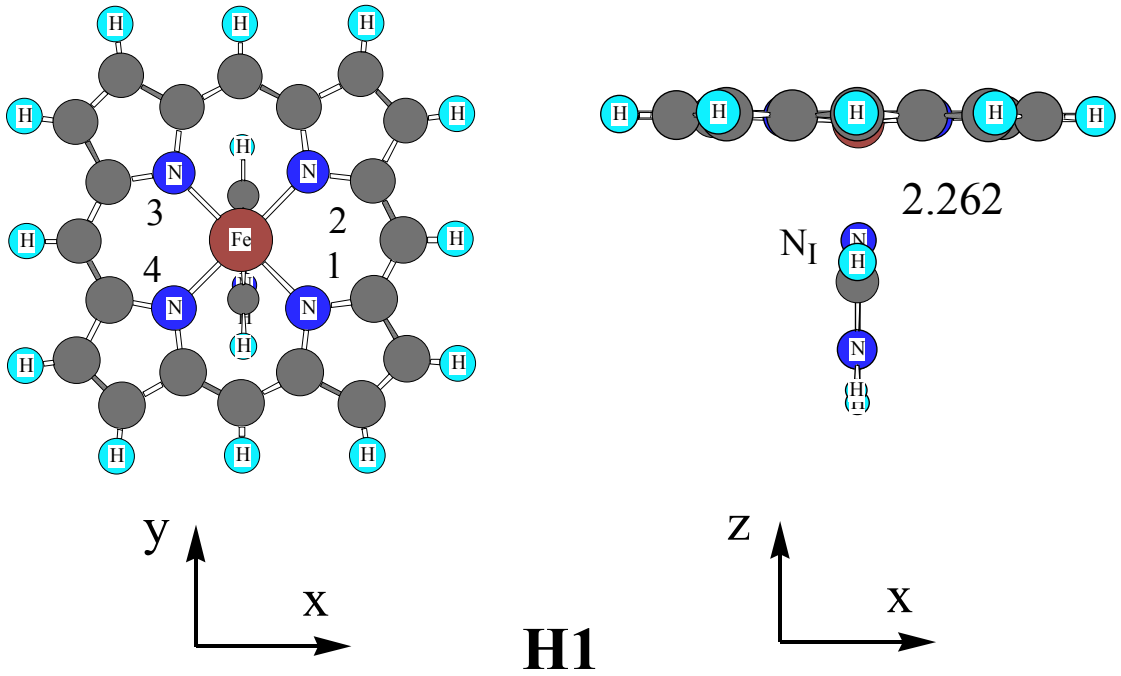

Figure 2. Heme model with the coordinate system. This is actually an optimized geometry of the triplet state.

The unrestricted solution of the SCF procedure of the open system with the antiferromagnetic spin coupling suffers from spin contamination from the next higher spin state. The spin contamination could be approximately removed for the spin–open state with the spin multiplicity of 2S+1, as follows [27–29]:

$$ {}^{2S+1}E_{PU} = {}^{2S+1}E_U + \frac{{}^{2S+1}\langle S^2\rangle_U - {}^{2S+1}\langle S^2\rangle}{{}^{2(S+1)+1}\langle S^2\rangle_U - {}^{2S+1}\langle S^2\rangle_U}({}^{2S+1}E_U - {}^{2(S+1)+1}E_U) \quad (1) $$

Here, ${}^{2S+1}E_{PU}$ is an approximately projected energy of the desired spin state of 2S+1, ${}^{2S+1}E_U$ is an unrestricted B3LYP (UB3LYP) energy of the 2S+1 state, and ${}^{2S+1}\langle S^2\rangle_U$ is a spin angular momentum of UB3LYP.

3 RESULTS AND DISCUSSION

According to the process shown in Scheme 1 (A), we added sequentially protons and an electron to the heme **H1** shown in Figure 2, as follows: (1) Addition of a triplet O_2 molecule to **H1**, giving an oxy heme complex Fe–OO, **H2**. (2) Addition of a proton to **H2**, giving a hydroperoxy heme complex FeOOH, **H3**, with the same spin state as **H2**. (3) Addition of an electron to **H3**, giving a hydroperoxy heme complex FeOOH, **H4**, with the different spin state from **H3**. (4) Addition of a proton to **H4**, giving an oxo heme complex Fe=O and a H_2O molecule, **H5**. The optimized structures of **H2**, **H3**, **H4**, and **H5** are summarized in Figure 3. The OO bond axes of all structures lie on the xz–plane. The energetics and spin angular momentums of all heme complexes are summarized in Table 1, and also the key bond distances and angle are summarized in Table 2.

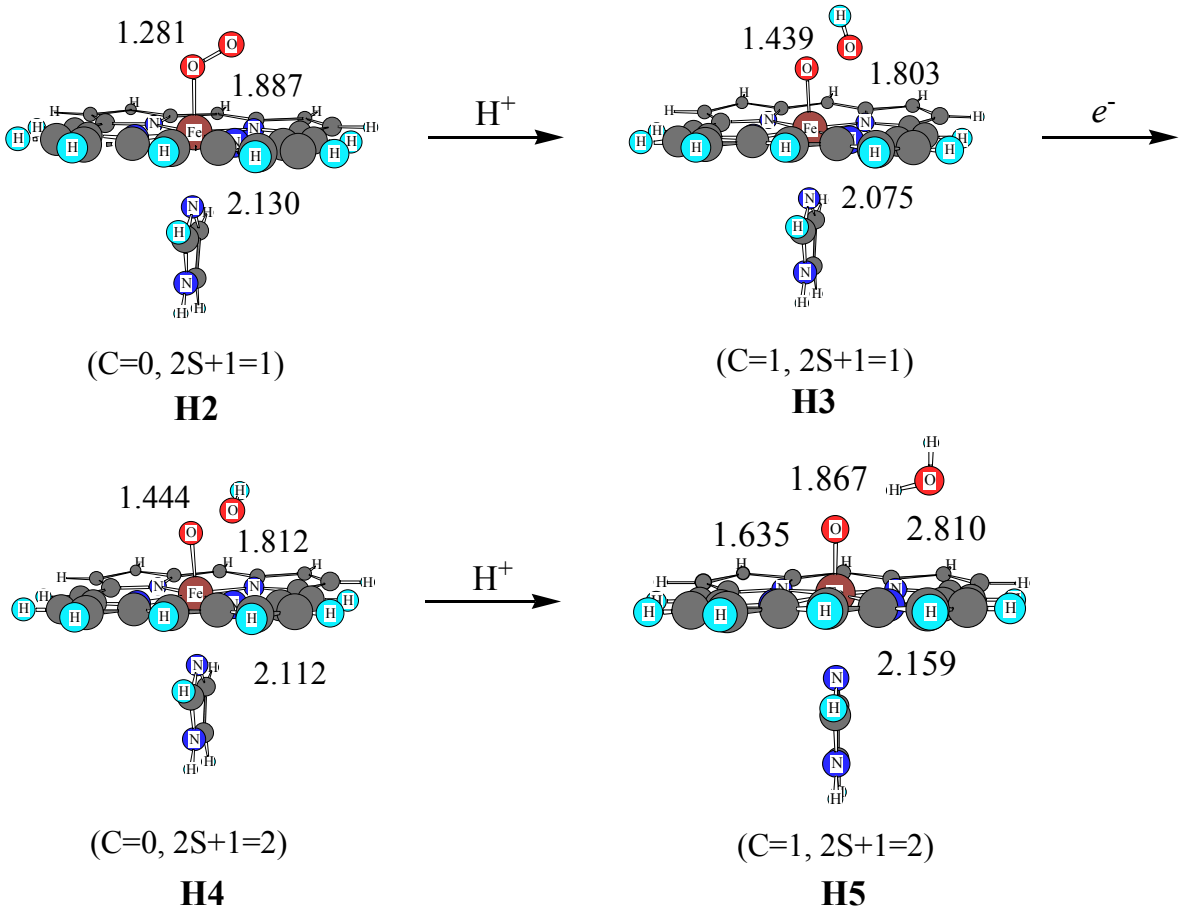

Figure 3. Optimized geometries of heme(Fe)–dioxygen complexes. The C values in parentheses mean the total charge of the systems. Bond distances are given in unit of Å.

The ground state of the oxy heme **H2** is an open singlet state with 5.4 kcal/mol lower in energy than the triplet state **H2'**, as shown in Table 1. The approximate projection to the pure singlet spin state gives the binding energy of 15.6 kcal/mol, comparable with 15 kcal/mol estimated by Rovira *et al*. [30–32]. The OO distance of 1.281 Å is similar to 1.30 Å of Rovira *et al*., while the Fe–N_I and

Fe–O distances of 2.130 Å and 1.887 Å are longer by 0.05 Å and 0.12 Å than those of Rovira *et al*., respectively.

Table 1. Total energies (au), spin angular momentums (au), and relative energies (kcal/mol) of optimized heme(Fe)–dioxygen complexes

Interm.	Spin States	E_{total}	$<S^2>$	ΔE_{rel}
H1	Triplet	–2478.340573	2.0601	
O_2	Triplet	–150.370417	2.0088	
H1 + O_2		–2628.710991		0.0
H2	Singlet	–2628.726544	1.0084	–9.8
	Projected [a]	–2628.735812		–15.6
H2'	Triplet	–2628.718168	2.0322	–4.5
H3	Singlet	–2629.122166	1.0533	
	Projected [a]	–2629.122425		
H4	Doublet	–2629.342425	0.7698	
H5	Doublet	–2629.771392	1.7889	
	Projected [a]	–2629.771394		

[a] Approximately projected energies estimated by using Eq. (1).

Table 2. Optimized geometrical parameters of heme(Fe)–dioxygen complexes

Intm.	Fe–N1	Fe–N2	Fe–N3	Fe–N4	Fe–N_I[a]	Fe–O	O–O	O–H	Fe–O–O
H1	2.010	2.008	2.008	2.010	2.262				
H2	2.011	2.009	2.022	2.024	2.130	1.887	1.281		119.6
H3	2.009	2.008	2.026	2.028	2.075	1.803	1.439	0.971	114.4
H5	2.011	2.012	2.026	2.026	2.112	1.812	1.444	0.971	115.0
H4	2.021	2.020	2.020	2.020	2.159	1.635	2.810	1.867[b]	118.2

[a] Nitrogen atom in imidazole. [b] Distance between O in FeO and H in H_2O.

Table 3. Charge (ρ) and spin (σ) populations of atoms and moieties in **H2** and C*c*O**1** estimated by the natural bond orbital analyses. Por and Imz mean a porphyrin ring and an imidazole moiety, respectively

Interm.	**H2**		C*c*O**1**	
(C, 2*S*+1)	(0,1)		(1,1)	
	ρ	σ	ρ	σ
Fe	1.642	1.197	1.627	1.054
Por	–1.260	–0.049	–1.183	–0.049
Imz	0.103	0.001	0.149	0.009
OO	–0.486	–1.149	–0.563	–0.996
Cu			0.820	–0.015

The spin angular momentum of 1.0084 shows that spins of the unpaired electrons couple in an antiferromagnetic manner. Table 3 shows the charge and spin populations estimated by the natural bond orbital calculations [33,34] for **H2** and C*c*O**1**. Porphyrin ring has charge density of –1.260 *e* rather than formal charge of –2.0 *e*, the dioxygen (OO) has large negative charges of –0.486 *e*, and Fe–atom has 1.642 *e*. Those indicate that the electron charges transfer from porphyrin to Fe and from Fe to OO. From the spin densities in Table 3, the antiferromagnetically coupled electrons are localized on Fe with an up–spin and OO with a down–spin, indicating that **H2** is a singlet biradical

state with the oxidation state of Fe(III). The resulting electronic structure is well coincide with those obtained by Rovira et al. [30–32]. The electron occupations of the singly occupied molecular orbital (SOMO–1 and SOMO+1) shown in Table 5 give a weak biradical character of 0.424. This antiferromagnetic spin coupling is caused by the bonding and antibonding interactions of d_{yz} of Fe and π_y* of OO. As can be seen from Table 3, the electronic structure of **H2** is essentially identical with that of Fe–OO moiety in the oxy intermediate C*c*O**1**.

The addition of a proton to **H2** increases the total charge of the system by unity and does not change the spin state from the singlet state. The $<S^2>$ value of **H3** is estimated to be 1.0533, indicating the possibility that the antiferromagnetic spin coupling exists because of increasing by unity from $< S^2>=0$ of the pure singlet state. The bond distances of O–O and Fe–O are 1.439 Å and 1.803 Å, which are remarkably increased and decreased by the proton addition, respectively. As shown in Table 4, the negative charges of the porphyrin are remarkably decreased from –1.260 *e* to –0.313 *e*, while the charge densities on Fe and OOH (OO in **H2**) are unchanged. It seems that an electron of the porphyrin transferred to OOH attached by the proton, being consistent with that the spin densities on OOH and on the porphyrin are vanished and appeared, respectively.

Table 4. Charge (ρ) and spin (σ) populations of atoms and moieties in **H3**, **H4**, **H5**, C*c*O**2**, and C*c*O**3** estimated by the natural bond orbital analyses.

Interm.	**H3**		**H4**		C*c*O**2**		C*c*O**3**		**H5**	
(C, 2*S*+1)	(1,1)		(0,2)		(2,1)		(1,2)		(1,2)	
	ρ	σ	ρ	σ	ρ	σ	ρ	σ	ρ	σ
Fe	1.636	–0.843	1.663	–0.965	1.638	0.959	1.627	–0.930	1.670	–1.282
Por	–0.313	1.036	–1.255	0.043	–0.908	–0.322	–1.216	0.049	–0.162	1.056
Imz	0.141	0.019	0.107	0.007	0.161	–0.006	0.130	0.002	0.124	0.019
OOH	–0.464	–0.212	–0.515	–0.084	–0.560	0.069	–0.518	–0.122		
O									–0.616	–0.789
H_2O									–0.016	–0.004
Cu					1.177	–0.504	0.722	–0.000		

Table 5. Electron occupations of natural orbitals for heme(Fe)–dioxygen complexes.

	H2	**H3**	**H4**	**H5**
LUMO	0.051	0.009	0.007	0.005
SOMO+1	0.683	0.997		0.996
SOMO			1.0	1.0
SOMO–1	1.317	1.003		1.004
HOMO	1.949	1.991	1.993	1.995

As can be found from Figure 3, it is interesting that FeOOH in **H3** lies on the xz–plane. Accordingly, the vacant 1s orbital of the proton strongly interacts with d_{z^2} (Fe) + π_z*(OO), which is a HOMO of **H2**, forming the bonding orbital d_{z^2} (Fe) + π_z*(OO) + 1s(H) with large charge transfer from Fe (d_{z^2}) to H (1s). The resulting antibonding orbital d_{z^2} (Fe) + π_z*(OO) – 1s(H) interacts with

the doubly occupied π orbital of the porphyrin ring to form the bonding orbital with the large electron weight on the porphyrin ring. The formed orbital lies in energy above the d_{yz}(Fe) + π_y*(OO), which is SOMO–1 in **H2**. Then the d_{yz}(Fe) + π_y*(OO) orbital is changed from singly occupied to doubly occupied orbital with the electron transfer from the π orbital of the porphyrin. Therefore, the antiferromagnetic spin coupling orbitals, SOMO–1 and SOMO+1 are composed of the π orbital of the porphyrin and d_{yz}(Fe) – π_y*(OO), as can be seen from Figure 4. The electron occupations in Table 5 gives biradical character of 0.994, showing strong antiparallel spin coupling of the unpaired electrons localized on Fe and porphyrin ring. The electron transfer where the d_{yz}(Fe) + π_y*(OO) is changed to the doubly occupied orbital enhances the bonding character of Fe–O and the antibonding character of OO, thus consistent with the FeO bond distance decreased by 0.084 Å and the OO bond distance increased by 0.158 Å compared with those of **H2**.

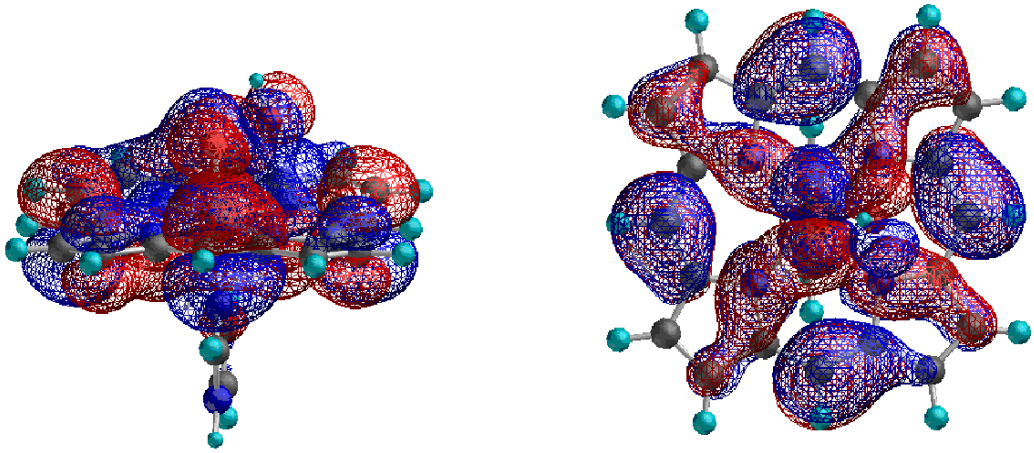

SOMO–1 SOMO+1

Figure 4. Natural orbitals corresponding to the antiferromagnetic spin coupling for hydroperoxy heme complex **H3**.

It is also interesting to compare with the electronic structure of C*c*O**2**, in which FeOOH on heme a_3 is formed by addition of a proton. The charge and spin densities of Fe and OOH in C*c*O**2** are similar to **H3**, while the spin densities of the porphyrin decreases from 1.036 *e* to 0.322 *e* with increasing the negative charge from –0.313 *e* to –0.908 *e*. The spin density on Cu is also grown up to 0.504 *e*, showing the change of the oxidation state of Cu from Cu(I) to Cu(II). It is clear that the Cu atom in the active site of C*c*O plays an important role for occupying the unpaired π orbital of the porphyrin of **H3** with the electron transfer from Cu to the porphyrin. It can be also seen that the bond characteristic of Fe–OOH in **H3** is similar to that of C*c*O**2**.

The addition of an electron to **H3** to yield **H4** changes the spin state from the single to doublet state. The $<S^2>$ value of **H4** is 0.7698 (Table 1) close to the value of the pure doublet spin state. From Table 4, the spin density of the porphyrin ring is disappeared, and the unpaired electron is

localized on Fe atom, giving that the oxidation state of Fe is still Fe(III). Thus, the additive electron occupies the unpaired π orbital of the porphyrin ring in **H3**. Our charge densities are considerably different from those obtained by the BP86 functional and DN** numerical basis set of Silaghi–Dumitrescu [35]. Interestingly, our conclusion that the oxidation state of Fe is Fe(III) is same as his conclusion.

The changes of the bond distances and angle of Fe–OOH moiety from **H3** to **H4** are definitely small. This indicates that the occupation of an electron into porphyrin ring does not alter significantly the bonding character of Fe–OOH moiety, consistent with the changes of charge and spin densities.

Compared with the electronic structures of C*c*O**3**, in which an electron is added to C*c*O**2** as shown in Scheme 1, the charge and spin densities of **H4** are perfectly same to those of C*c*O**3**. We can make a comment through discussion on the electronic structures of **H1**, **H2**, **H3**, and **H4**, and the comparisons with those of C*c*O**1**, C*c*O**2**, and C*c*O**3**. In considering the reduction mechanism in the active site of C*c*O, the examination of the naked heme only corresponding to heme a_3 moiety of the active site is effective.

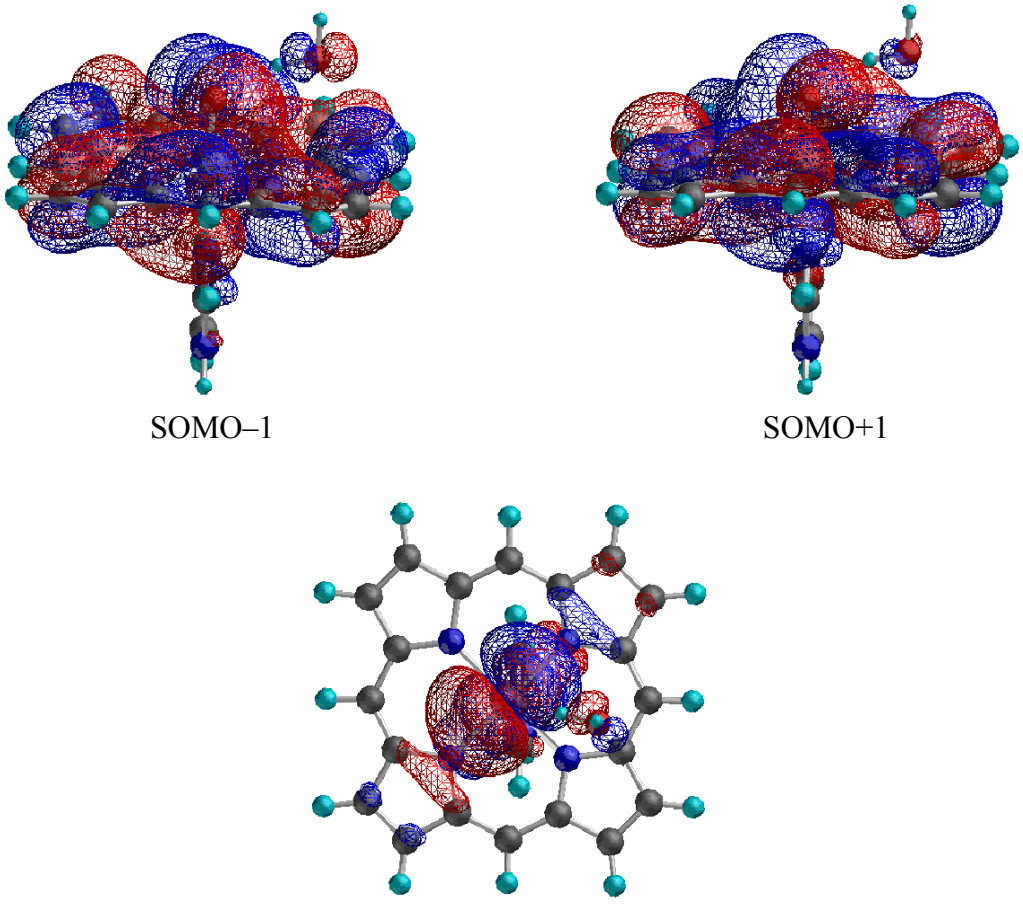

SOMO–1 SOMO+1

SOMO

Figure 5. Natural orbitals of oxo heme complex **H5**.

The second addition of a proton leads the OO bond cleavage, giving the structure **H5**, as shown in Figure 3. The H_2O molecule generated by the OO bond cleavage is hydrogen bonded to oxo heme. The distance between oxo (O) and O of H_2O is given in 1.867 Å (Figure 1 and Table 2), comparable to the standard hydrogen–bonding distance. The $<S^2>$ value shown in Table 1 is 1.7889, which is increased by unity from 0.75 of the pure doublet state, indicating that the pure unpaired spin and the antiferromagnetic coupling spins exist in the complex of oxo heme and H_2O. In fact, the antiferromagnetic coupling spins are confirmed by the electron occupations of SOMO–1 and SOMO+1, as can be seen in Table 5.

The spin densities of **H5** in Table 4 show two down–spins on FeO moiety and single up–spin on the porphyrin ring. From the charge and spin densities in Table 4, the single electron with the down–spin in the porphyrin ring moves to the $FeOOH_2$ moiety and occupy the antibonding orbital of $O–OH_2$ with the charge transfer to the OH_2 moiety, resulting in the OO bond cleavage to yield a H_2O molecule. Figure 5 shows the natural orbitals corresponding to SOMO–1, SOMO+1, and SOMO.

The SOMO, the pure unpaired electron, is composed of the antibonding interaction between d_{xz} on Fe and p_x on O, while the SOMO–1 and SOMO+1 are from the bonding and antibonding interaction of d_{yz} (Fe) – π_y (O) and π on the porphyrin. These pictures presents that the electronic structure of the oxo heme moiety corresponds to that of a compound I, an Fe(IV)–porphyrin radical cation, as an intermediate of enzyme catalytic reactions such as peroxidase and catalase [36–38].

The Fe–O distance is estimated to be 1.635 Å, remarkably shortened from that of **H4**. However, this value is comparable with 1.64–1.70 Å determined by experiments [39,40], and with 1.669 Å of theoretical value [38]. As can be seen from Table 1, the approximate projection to the pure doublet state does not yields remarkable energy lowering, meaning that the quartet state with three unpaired spins on FeO and Por is degenerate with the doublet state. In fact, the optimized geometry of the quartet state (not shown here) gives –2629.771438 au of total energy. The energy difference of the doublet and quartet states are only 0.03 kcal/mol, consistent with 0.07 kcal/mol for oxo heme model of compound I [38].

In introduction, we described that the OO bond cleavage does not occurs and the OO distance falls in 1.484 Å for examining the O_2 reduction mechanism in the active site of C*c*O, conflicting with the OO bond cleavage observed for heme(Fe)–dioxygen complex. Judging from the consideration that the heme(Fe)–dioxygen complex represents well the electronic structure of heme a_3, we have to reexamine the mechanism of the OO bond cleavage in active site of C*c*O. Probably,

the OO bond in $FeOOH_2$ shown in Scheme 1(A) intrinsically has the ability to cleave the OO bond with the small activation energy. It also seems that the $FeOOH_2$ is a transient intermediate to yield a H_2O molecule in the reduction of O_2 molecule. The final stage of forming Fe=O might be a [Fe=O, H_2O, Cu(I)] with a compound I or a [Fe=O, H_2O, Cu(II)] with a compound II. We are now reexamining the mechanism of the reduction of O_2 in C*c*O.

In Scheme 1(A), the addition of an electron from C*c*O**2** to C*c*O**3** is available for the reduction mechanism in the fully reduced C*c*O not in the mixed valence C*c*O. Since two electrons are already provided to the active site by changing from the oxidized form [Fe(III), Cu(II)] to the reduced form [Fe(II), Cu(I)] at the first stage of the reaction, no more electron cannot be added in the active site of the mixed valence C*c*O. The change from C*c*O**2** to C*c*O**3** causes the reduction of Cu atom without altering the bonding character of FeOOH, as can be seen from Table 4. Thus, it seems that the electronic structure of heme a_3 of C*c*O**2** is similar to that of C*c*O**3**. Accordingly, the electronic structure of heme a_3 of C*c*O**2** is similar to that of **H4** because of that the **H4** corresponds to heme a_3 of C*c*O**3**. These indicate the possibility that the addition of the second proton to C*c*O**2** leads the OO bond cleavage with maintaining the oxidation state of Cu(II) and changing from the neutral porphyrin to the radical cationic porphyrin by electron transfer to $FeOOH_2$, as shown in Scheme 2. This consideration should be also examined.

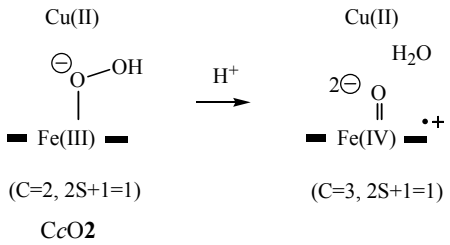

Scheme 2. Proposal for the O_2 reduction mechanism in the mixed valence C*c*O.

4 CONCLUSIONS

In this report, the electronic structures of the protonated heme(Fe)–dioxygen complexes as an intermediate models of dioxygen reduction in C*c*O are examined by using the unrestricted hybrid–correlation functional B3LYP method. It was shown that the protonated heme(Fe)–dioxygen complexes is effective models for considering the mechanisms in both fully reduced and mixed valence C*c*O. Our results obtained in this study are summarized as follows:

1) The proton addition to FeOO (**H2**) to yield FeOOH (**H3**) causes the electron transfer from the porphyrin ring to FeOOH moiety, giving the porphyrin radical cation, which is changed to the

neutral porphyrin by altering from Cu(I) to Cu(II) in the C*c*O.

2) The proton addition to FeOOH (**H4**) leads to the OO bond cleavage, yielding the hydrogen bonded complex of an oxo heme (compound I) and a H_2O molecule.

3) The bonding characters of FeOOH in **H3** and **H4** are identical, even the electronic structures of the porphyrin rings in **H3** and **H4** are different. However, The proton addition to FeOOH (**H3**) does not lead to the OO bond cleavage, since the electron transfer from porphyrin–radical cation in **H3** to $FeOOH_2$ needs the high energy.

4) Our results support the proposal of Faxén and co–workers. We have to reexamine our mechanism of the OO bond cleavage in active site of C*c*O. The protonated heme(Fe)–dioxygen complexes is effective models for considering the mechanisms in both fully reduced and mixed valence C*c*O.

Acknowledgment

This work was supported by The Japanese Ministry of Education, Science, and Culture.

5 REFERENCES

[1] B. G. Malmstörm, *Chem*. *Rev*. **1990**, *90*, 1247–1260.
[2] G. T. Babcock and M. Wikstörm, *Nature* **1992**, *356*, 301–309.
[3] S. Furguson–Miller and G. T. Babcock, *Chem*. *Rev*. **1996**, *96*, 2889–2907.
[4] T. Tsukihara, H. Aoyama, E. Yamashita, T. Tomizaki, H. Yamaguchi, K. Sinzawa–Itoh, R. Nakashima, R. Yaono, S. Yoshikawa, *Science* **1995**, *269*, 1069–1074
[5] T. Tsukihara, H. Aoyama, E. Yamashita, T. Tomizaki, H. Yamaguchi, K. Sinzawa–Itoh, R. Nakashima, R. Yaono, S. Yoshikawa, *Science* **1996**, *272*, 1136–1144.
[6] S. Yoshikawa, K. Sinzawa–Itoh, R. Nakashima, R. Yaono, E. Yamashita, N. Inoue, M. Yao, M. J. Fei, C. P. Libeu, T. Mizushima, H. Yamaguchi, T. Tomizaki, and T. Tsukihara, *Science* **1998**, *280*, 1723–1729.
[7] T. Tsukihara, K. Shimokata, Y. Katayama, H. Shimada, K. Muramoto, H. Aoyama, M. Mochizuki, K. Shinzawa–Itoh, E. Yamashita, M. Yao, Y. Ishimura, and S. Yoshikawa, *Proc*. *Natl*. *Acad*. *Sci*. *USA* **2003**, *100*, 15304–15309.
[8] D. A. Proshlyakov, M. A. Pressler, C. DeMaso, J. F. Leykam, D. L. DeWitt, and G. T. Bacock, *Science* **2000**, *290*, 1588–1591.
[9] M. Fabin, W. W. Wong, R. B. Gennis, and G. Palmer, *Proc*. *Natl*. *Acad*. *Sci*. *USA*. **1999**, *96*, 13114–13117.
[10] D. A. Proshlyakov, T. Ogura, K. Sinzawa–Itoh, S. Yoshikawa, E. H. Appelman, and T. Kitagawa, *J*. *Biol*. *Chem*. **1994**, *269*, 29385–29388.
[11] D. A. Proshlyakov, T. Ogura, K. Sinzawa–Itoh, S. Yoshikawa, and T. Kitagawa, *Biochemistry* **1996**, *35*, 8580–8586.
[12] M. Aki, T. Ogura, K. Sinzawa–Itoh, S. Yoshikawa, and T. Kitagawa, *J*. *Phys*. *Chem*. *B* **2000**, *104*, 10765–10774.
[13] D. A. Proshlyakov, M. A. Pressler, and G. T. Babcock, *Proc*. *Natl*. *Acad*. *Sci*. *USA*. **1998**, *95*, 8020–8025.
[14] J. E. Morgan, M. I. Verkhovsky, G. Palmer, and M. Wikström, *Biochemistry* **2001**, *40*, 6882–6892.
[15] M. Svensson–Ek, J. W. Thomas, and R. B. Gennis, T. Nilson, and P. Brzezinski, *Biochemistry* **1996**, *35*, 13673–13680.
[16] P. Brzezinski and P. Adelroth, *Bioenerg*. *Biomembr*. **1998**, *30*, 99–106.
[17] Y. Yoshioka, H. Kawai, and K. Yamaguchi, *Chem*. *Phys*. *Lett*. **2003**, *374*, 45–52.

[18] Y. Yoshioka and M. Mitani, *Internet Electron. J. Mol. Des.* **2003**, *2*, 732–740.
[19] Y. Yoshioka and H. Kawai, manuscript in preparation.
[20] K. Faxén, G. Gilderson, P. Ädelroth, and P. Brzezinski, *Nature* **2005**, *437*, 286–289.
[21] A. D. Becke, *J. Chem. Phys.* **1993**, *98*, 1372–1377.
[22] A. D. Becke, *J. Chem. Phys.* **1993**, *98*, 5648–5652.
[23] A. D. Becke, *Phys. Rev.* **1998**, *A38*, 3098–3100.
[24] P. J. Stevens, F. J. Devlin, C. F. Chablowski, and M. J. Frish, *J. Phys. Chem.* **1994**, *98*, 11623–11627.
[25] A. J. H. Wachters, *J. Chem. Phys.* **1970**, *52*, 1033–1040.
[26] M. J. Frish, *et al*., GAUSSIAN 98, Revision A.6, Gaussian Inc., Pittsburgh, PA, **1998**.
[27] Y. Yoshioka, D. Yamaki, G. Maruta, T. Tsunesada, K. Takada, T. Noro, and K. Yamaguchi, *Bull. Chem. Soc. Jpn.* **1996**, *69*, 3395–3415.
[28] M. Nishino, S. Yamanaka, Y. Yoshioka, and K. Yamaguchi, *J. Phys. Chem.* **1997**, *101*, 705–712
[29] Y. Yoshioka, D. Yamaki, S. Kiribayashi, T. Tsunesada, M. Nishino, K. Yamaguchi, K. Mizuno, and I. Saito, *Electronic J. Theoret. Chem.* **1977**, *2*, 218–235.
[30] C. Rovira, P. Ballone, and M. Parrinello, *Chem. Phys. Lett.* **1997**, *271*, 247–250.
[31] C. Rovira, K. Kunc, J. Hutter, P. Ballone, and M. Parrinello, *Int. J. Quantum Chem.* **1998**, *69*, 31–35.
[32] C. Rovira, K. Kunc, J. Hutter, P. Ballone, and M. Parrinello, *J. Phys. Chem. A* **1997**, *101*, 8914–8925.
[33] A. E. Reed, R. B. Weinstock, and F. Weinhold, *J. Chem. Phys.* **1985**, *83*, 735–746.
[34] A. Reed, L. A. Curtiss, and F. Weinhold, *Chem. Rev.* **1988**, *88*, 899–926.
[35] R. Silaghi–Dumitrescu, *Archives Biochem. Biophys.* **2004**, *424*, 137–140.
[36] A. Ivancich, H. M. Jouve, and J. Gaillard, *Biochemistry* **1997**, *36*, 9356–9364.
[37] C. Rovira and I. Fita, *J. Phys. Chem B* **2003**, *107*, 5300–5305.
[38] E. Derat, S. Cohen, S. Shaik, A. Altun, and W. Thiel, *J. Am. Chem. Soc.* **2005**, *127*, 13611–13621.
[39] M. Chance, L. Powers, T. Poulos, and B. Chance, *Biochemistry* **1986**, *25*, 1266–1270.
[40] G. I. Berglund, G. H. Carlsson, A. T. Smith, H. Szoeke, A. Henriksen, and J. Hajdu, *Nature* **2002**, *417*, 463–468.

Biographies

Yasunori Yoshioka is professor of chemistry at Mie University. After obtaining a Ph.D. degree in quantum chemistry from Osaka University, Dr. Yoshioka undertook postdoctoral research with Professor Kenneth D. Jordan at the University of Pittsburgh and Professor Henry F. Schaefer III at the University of California, Berkeley.

Masaki Mitani is associate professor of chemistry at Mie University, and obtained a Ph.D. degree in quantum chemistry from Hiroshima University.

Hiroyuki Satoh is graduate student at Mie University.